Raman Optical Activity of Methyloxirane Gas and Liquid

ARTICLE *in* JOURNAL OF PHYSICAL CHEMISTRY LETTERS · FEBRUARY 2011

Impact Factor: 7.46 · DOI: 10.1021/jz200108v

THE JOURNAL OF PHYSICAL CHEMISTRY Letters

LETTER

pubs.acs.org/JPCL

Raman Optical Activity of Methyloxirane Gas and Liquid

Jaroslav Šebestík* and Petr Bouř*

Department of Molecular Spectroscopy, Institute of Organic Chemistry and Biochemistry, Academy of Sciences, Flemingovo náměstí 2, 166 10 Prague, Czech Republic

Supporting Information

ABSTRACT: Raman and Raman optical activity spectra (ROA) of methyloxirane enantiomers were measured in neat liquid and gas phases and compared with quantum chemical computations. Simulated rotational line broadening for the gas corresponded to the observations. The differences in vibrational frequencies caused by the self-solvation calculated with the use of a continuum model well corresponded to the experimental ones. Anharmonic corrections improved the harmonic frequencies and intensities. The comparison of the gaseous and liquid state data is useful for benchmark studies of molecular interactions with environment. The ROA spectroscopy provides additional information to the Raman scattering and makes the mode assignment more reliable.

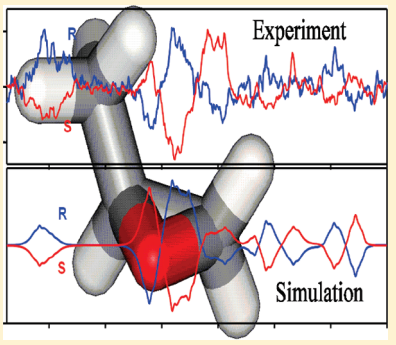

SECTION: Kinetics, Spectroscopy

The spectroscopy of Raman optical activity (ROA) measures tiny differences in the Raman scattering of left and right circularly polarized light. The first spectrum was measured in 1973,[1] and the method was soon established as a useful probe into the structure and conformational behavior of molecules.[2] In particular, biologically relevant systems, such as peptides,[3−5] proteins,[6,7] nucleic acids,[8] and even viruses,[9] can be conveniently measured in the natural aqueous environment. The method is very sensitive to molecular flexibility[10] and has a potential to be combined with a surface enhancement on metal surfaces.[11,12]

However, the circular intensity difference (CID), the ratio of the ROA difference to the total scattered radiation,[13] is usually very small, $\sim 10^{-4}$, and advanced setups are required to avoid artifacts in measured signal.[14−17] Unlike for the vibrational circular dichroism (VCD, which is another common form of vibrational optical activity), fluorescence phenomena often inhibit collection of ROA spectra and restrict the application span. Therefore, for example, whereas solid[18] and gaseous[19] VCD techniques for molecules exist, only a crystal ROA[20] was reported so far. Purely rotational ROA was found to be possible theoretically,[21] but it is not available because of limited instrumental resolution and frequency range. This again contrasts with the infrared techniques, where the rotational resolution was achieved at least for the magnetic VCD.[22]

We found that it was possible to collect the ROA gaseous spectra on a commercial apparatus in a longer sample cell if the signal coming from the cell-fused silica window could be subtracted. One way to do it is to let the sample vapor gradually escape during the measurements so that the cell does not change orientation between the sample and baseline signal collection.

The gas spectroscopic response is useful to benchmark theoretical studies. The ROA applications were to a large extent triggered by reliable computations that could be used to interpret the spectra.[23] The vibrational optical activity of substituted oxiranes in the liquid case was previously investigated for the large signal and molecular rigidity.[24] Introduction of gauge-invariant atomic orbitals[25] and analytical coupled-perturbed DFT techniques[26,27] accelerated the calculations and made them accessible for larger molecules.[28,29] For small peptides, the same conformer ratios could be obtained from ROA as from NMR spectra, providing accurate simulations were available.[30] Nevertheless, anharmonic interactions can significantly lower the precision of the simulations,[31] and solvation effects are difficult to model theoretically.[32] Comparison of the spectra obtained in many environments, including vacuum, can thus help us to validate the theoretical approaches, and, in a final effect, to understand the intermolecular interactions.

Because the *S*- and *R*-methyloxirane liquid Raman and ROA spectra were analyzed before, including the band assignment,[24] we concentrate on the vapor. The experimental Raman of *S*-methyloxirane is presented in Figure 1. Note that the absolute intensity is impractical to measure because it depends on the accumulation time, laser power, and so on. The relative intensities approximately correspond to the liquid experiment;[24] however, they are significantly broadened by the rotational motion. Also, a fine rotational structure is apparent, including the P, Q, and R branches,[33] which is unfortunately impossible to resolve fully on the ROA spectrometer, where one pixel row of the CCD detector covers ~ 3 cm^{-1}.

Nevertheless, the simulations (Figure 1) reasonably well-reproduce the intensity distribution within the entire range of wavenumbers. Also, we can see that the 30 K spectrum (blue in Figure 1) exhibits the rotational broadening too narrow, whereas 300 K (red curve) is more realistic. The simulation of the

Received: January 23, 2011
Accepted: February 8, 2011
Published: February 15, 2011

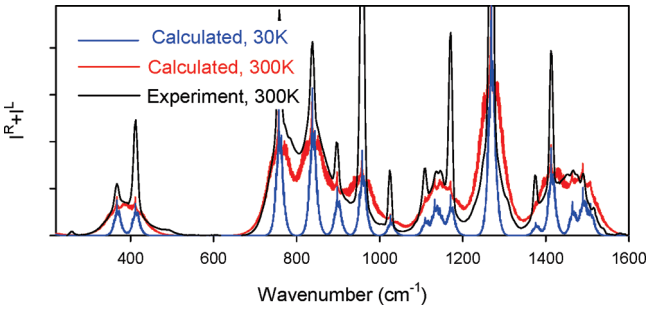

Figure 1. Raman spectrum of *S*-methyloxirane: the vibrational−rotational envelopes simulated for two temperatures and the experiment at 300 K. The symmetric top approximation and the B3LYP/aug-cc-pVTZ intensities were used for the simulations, with frequencies scaled according to the experiment.

temperature dependence also gives us an important feedback about the quality of the spectra, which can be easily destroyed, for example, by an accidental irradiation of the detector during the measurement.

In Table 1, calculated and vapor experimental *S*-methyloxirane frequencies are compared, and the average absolute deviations are listed. The MP2 frequencies computed previously (δ = 50 cm^{-1})[24] are significantly improved by using the larger basis set in this study (δ = 21 cm^{-1}); still, the B3LYP method provides more accurate results (δ = 15 cm^{-1}). The remaining error can be further reduced by the inclusion of the anharmonic interaction, either by the perturbation (δ = 12 cm^{-1}) or by a more advanced VCI (δ = 7 cm^{-1}) method. Note that the first mode (methyl-rotation) was not included in the anharmonic corrections because its potential is strongly anharmonic. In this case, an adiabatic approximation would have to be used,[34] which goes beyond the goal of this study. The higher frequency modes do significantly profit from the anharmonic correction, which is also documented in Figure 2, where harmonic, anharmonic (VCI), and the experimental Raman spectra are plotted. For most modes, the anharmonic positions are closer to experiment. Within 1300−1600 cm^{-1}, the anharmonic correction even leads to a much more realistic intensity distribution. Calculated Raman intensities of combination bands are small and with the current sensitivity of the instrument not reliably detectable; nevertheless, a weak signal at ∼800 cm^{-1} and above 1500 cm^{-1} indicates such bands, both in theory and in experiment.

The *S*- and *R*-methyloxirane vapor ROA spectra are plotted in Figure 3, and compared with the simulated spectra (B3LYP/aug-cc-pVTZ intensities) and neat liquid ROA. Although the noise in the experimental gaseous ROA is much larger than that for the liquid, we can see that the *S*- and *R*-enantiomers provide reasonably symmetric (opposite) signals and that the strongest bands can readily be supported by the theory, including the rotational broadening. Relative intensities around 390 and 950 cm^{-1} are somewhat larger than those for the simulation or the liquid, but the sign pattern is probably identical. Unfortunately, the gaseous signal is obscured by noise within 1100−1600 cm^{-1} despite the absence of the cell window scattering in this region.

The similarity of the gaseous and liquid spectra reflects the tight link between the ROA intensities and the geometry.[23] A finer solvent effect on the intensities, also indicated for some systems,[35,36] cannot be estimated because of the larger noise in the vapor experiment. However, the solvatochromic Raman frequency shifts can be accurately evaluated from the gaseous and liquid experiments. These reasonably well correlate with the calculated shifts, as can be seen from the comparison in Figure 4. The shifts are similar to those obtained for acetonitrile as a solvent.[35] Most of the fundamental frequencies are shifted down

Table 1. Calculated and Experimental Fundamental Transition Frequencies of *S*-Methyloxirane

			B3LYP[b]			
mode	MP2[a]	MP2[b]	harm	Ah-PT2	Ah-VCI	exp
1	218	218	209	209	209	213
2	373	369	367	364	370	367
3	419	406	410	408	413	412
4	799	776	771	748	760	757
5	882	859	842	820	833	838
6	935	910	908	883	889	898
7	1006	977	973	948	958	958
8	1070	1048	1043	1017	1022	1026
9	1160	1127	1129	1102	1108	1109
10	1178	1154	1157	1124	1133	1133
11	1203	1171	1166	1138	1145	1145
12	1225	1194	1189	1162	1169	1171
13	1330	1296	1293	1264	1276	1269
14	1458	1404	1407	1369	1375	1376
15	1498	1451	1438	1397	1408	1413
16	1546	1499	1484	1435	1433	1464
17	1561	1514	1497	1454	1460	1490
18	1588	1537	1528	1483	1493	1508
δ[c]	50	21	15	12	7	0

[a] 6-31G* basis, ref 24. [b] Aug-cc-pVTZ basis, this work. [c] Average absolute deviation, $\delta = (1/N)\ \Sigma_{i=1}^{N}\ |\omega^i_{\mathrm{calcd}} - \omega^i_{\mathrm{exp}}|$.

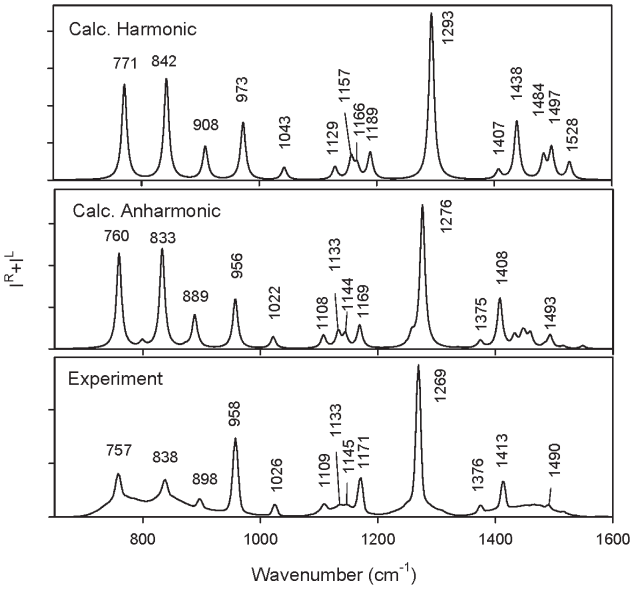

Figure 2. From top to bottom: calculated (B3LYP/aug-cc-pVTZ, Lorentzian profiles used only) harmonic and VCI anharmonic Raman spectra and the experimental spectrum of *S*-methyloxirane vapor. The calculated intensities were scaled arbitrarily by a common factor according to the experiment.

dx.doi.org/10.1021/jz200108v |*J. Phys. Chem. Lett.* 2011, 2, 498–502

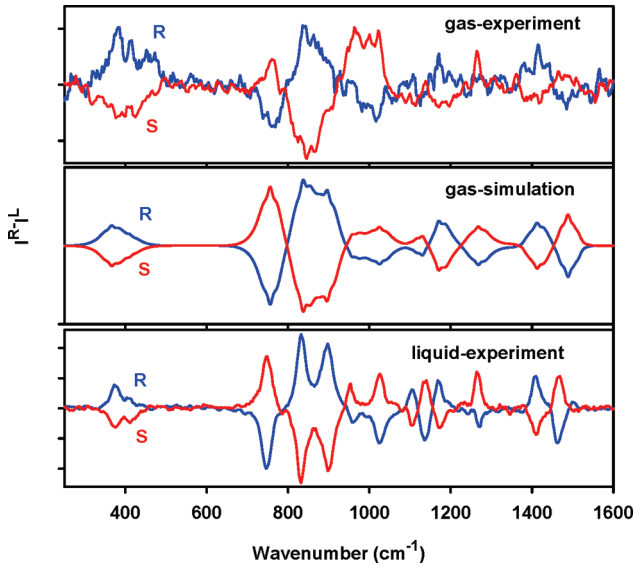

Figure 3. ROA spectra of the methyloxirane enantiomers, measured with vapor (top), simulated with the scaled B3LYP/aug-cc-pVTZ calculation (middle, frequencies scaled), and neat liquid (bottom). The *y* axis is arbitrary.

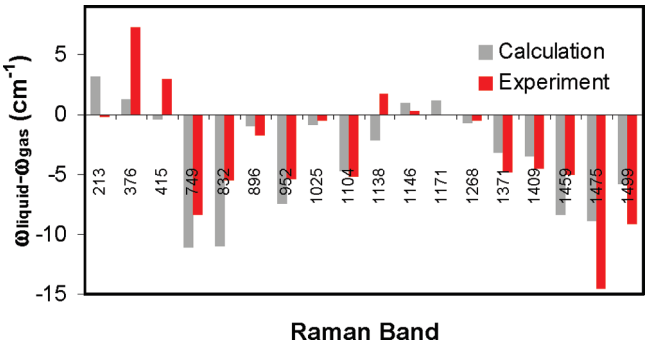

Figure 4. Comparison of calculated (B3LYP/aug-cc-pVTZ, vacuum vs CPCM) and experimental solvent shifts of fundamental *S*-methyloxirane Raman vibrational bands between the vapor and neat liquid spectra.

in the liquid, so that the force constants are weaker. As expected, the largest shifts occur at the C−O stretching region and for modes involving the oxygen (700−900 cm^{-1}).[24] Perhaps surprisingly, however, also the higher-frequency bands (>1300 cm^{-1}), involving most vibrations of the less polar molecular parts,[24] are affected. Nevertheless, all solvent shifts are rather small (<14 cm^{-1}) and cannot be compared, for example, with frequency changes caused by stronger interactions, such as hydrogen bonds, which often approach 100 cm^{-1}.[32]

We can thus conclude that the gaseous ROA measurement is possible with the available instrumental technique and that it can provide useful information about molecular structure, behavior, interaction with the environment, and the computational methodologies. The low sensitivity of the scattering technique remains a problem. Obviously, not all compounds can be measured as gases. The methyloxirane has a very low boiling point (33 °C), which allowed us to perform the measurement relatively easily in the room-temperature controlled by an air conditioning unit. The concentration of the vapors (~0.02 M) estimated from the oxygen and nitrogen partial pressures detected by the Raman intensity (Supporting Information) approximately corresponds to detection threshold in solutions and required days of accumulation time.[37] The larger concentration in the neat liquid (14.3 M) provided the spectra much faster (minutes) and with a smaller noise. Therefore, further improvements of the instrumentation are desirable for the ROA in the gas phase.

EXPERIMENTAL METHODS

The *S*- and *R*-methyloxiranes were purchased from Sigma and used without further purification. The spectra were measured with the Biotools μ-ChiralRAMAN-2X instrument, equipped with an Opus diode-pumped solid-state laser operating at 532 nm. Raman and ROA spectra of neat liquids were obtained in a fused silica cell of a total volume of 100 μL and optical path length of 1 mm. Gaseous spectra were obtained from the methyloxirane vapor when the liquid compound was partially filled and loosely sealed in a fused silica cell of a 1 cm path length, using laser power of 1600 mW (~800 mW at the sample) and illumination time of 8 s. After the sample evaporated (~1 to 2 days) the empty cell was used as a baseline. The evaporation was controlled by the intensity of the nonpolarized Raman scattering. (See the Supporting Information.) With a homemade program artifact "spikes" (false CCD detector signals, coming form cosmic rays, etc.) were removed. For the liquid sample spectra, no baseline correction was made; for the gas, the signal of the cell was subtracted, and a minor polynomial baseline correction was applied. For ROA, spectra of the R- and S-isomers were additionally averaged from two and three independent measurements, respectively, to exclude artifacts, in particular, the ROA components coming from the cell windows. No smoothing of the spectra was applied.

Calculations. The methyloxirane geometry was optimized by energy minimization using the Gaussian program[38] at the B3LYP[39]/aug-cc-pvTZ computational level. A larger aug-cc-pVQZ basis set was also tried, but it did not lead to significant changes in computed spectral parameters. The Raman and ROA spectra were calculated for the excitation frequency of 532 nm, with the default CP GIAO method.[27] For the neat liquid samples, the CPCM[40] continuum solvent model was adopted for the solvent correction, using the "solvent=tetrahydrofuran" option in Gaussian, which provided dielectric constant (refractive index n = 1.40) similar to that of the methyloxirane (n = 1.37). Backscattered intensities were generated by convolution with Lorentzian bands 5 cm^{-1} wide and the Boltzmann correction to the temperature of 300 K.[31,41] Rotational broadening of the spectral lines was simulated within the symmetric-top approximation[42] using adapted Vibrot program[43] from the CPC library (http://www.cpc.cs.qub.ac.uk/). For the gas spectra simulations (Figure 1, middle of Figure 4), the B3LYP/au-cc-pvTZ frequencies were replaced by the experimental ones; otherwise, no scaling was applied. Anharmonic corrections to the vibrational energies and intensities were calculated with the S4 program[44] interfaced to Gaussian using third and semidiagonal fourth energy derivatives,[31] the second-order degeneracy-corrected perturbation (PT2), and the vibrational configuration interaction (VCI) methods.[45] We considered 20 462 harmonic oscillator states for VCI. The calculated intensities were convoluted with a Lonrentzian function of the 5 cm^{-1} width that corresponds to the resolution of the instrument.

ASSOCIATED CONTENT

Supporting Information. Experimental details about baseline stability and the evaporation kinetics. The material is available free of charge via the Internet at http://pubs.acs.org.

AUTHOR INFORMATION

Corresponding Author
*E-mail: sebestik@uochb.cas.cz (J.S.), bour@uochb.cas.cz (P.B.).

ACKNOWLEDGMENT

This study was performed with the support from the Academy of Sciences (M200550902), Grant Agency of the Czech Republic (P208/11/0105), and the KONTAKT II MSMT program (LH11033).

REFERENCES

(1) Barron, L. D.; Bogaard, M. P.; Buckingham, A. D. Raman Scattering of Circularly Polarized Light by Optically Active Molecules. *J. Am. Chem. Soc.* **1973**, *95*, 603–605.

(2) Barron, L. D.; Zhu, F.; Hecht, L.; Tranter, G. E.; Isaacs, N. W. Raman Optical Activity: An Incisive Probe of Molecular Chirality and Biomolecular Structure. *J. Mol. Struct.* **2007**, *834*−*836*, 7–16.

(3) Zhu, F.; Isaacs, N. W.; Hecht, L.; Barron, L. D. Polypeptide and Carbohydrate Structure of an Intact Glycoprotein from Raman Optical Activity. *J. Am. Chem. Soc.* **2005**, *127*, 6142–6143.

(4) Kapitán, J.; Baumruk, V.; Kopecký, V., Jr.; Bouř, P. Demonstration of the Ring Conformation in Polyproline by the Raman Optical Activity. *J. Am. Chem. Soc.* **2006**, *128*, 2438–2443.

(5) McColl, I. H.; Blanch, E. W.; Hecht, L.; Kallenbach, N. R.; Barron, L. D. Vibrational Raman Optical Activity Characterization of Poly(L-proline) II Helix in Alanine Oligopeptides. *J. Am. Chem. Soc.* **2004**, *126*, 5076–5077.

(6) Barron, L. D.; Blanch, E. W.; Hecht, L. Unfolded Proteins Studied by Raman Optical Activity. *Adv. Protein Chem.* **2002**, *62*, 51–90.

(7) Syme, C. D.; Blanch, E. W.; Holt, C.; Jakes, R.; Goedert, M.; Hecht, L.; Barron, L. D. Raman Optical Activity Study of Rheomorphism in Caseins, Synucleins and Tau - New Insight into the Structure and Behaviour of Natively Unfolded Proteins. *Eur. J. Biochem.* **2002**, *269*, 148–156.

(8) Barron, L. D.; Hecht, L.; Blanch, E. W.; Bell, A. F. Solution Structure and Dynamics of Biomolecules from Raman Optical Activity. *Prog. Biophys. Mol. Biol.* **2000**, *73*, 1–49.

(9) Blanch, E. W.; McColl, I. H.; Hecht, L.; Nielsen, K.; Barron, L. D. Structural Characterization of Proteins and Viruses using Raman Optical Activity. *Vib. Spectrosc.* **2004**, *35*, 87–92.

(10) Kapitán, J.; Baumruk, V.; Kopecký, V., Jr.; Bouř, P. Conformational Flexibility of L-Alanine Zwitterion Determines Shapes of Raman and Raman Optical Activity Spectral Bands. *J. Phys. Chem. A* **2006**, *110*, 4689–4696.

(11) Abdali, S. Observation of SERS Effect in Raman Optical Activity, a New Tool for Chiral Vibrational Spectroscopy. *J. Raman Spectrosc.* **2006**, *37*, 1341–1345.

(12) Osinska, K.; Pecul, M.; Kudelski, A. Circularly Polarized Component in Surface-Enhanced Raman Spectra. *Chem. Phys. Lett.* **2010**, *496*, 86–90.

(13) Barron, L. D. *Molecular Light Scattering and Optical Activity*; Cambridge University Press: Cambridge, U.K., 2004.

(14) Nafie, L. A.; Che, D. Theory and Measurement of Raman Optical Activity. In *Modern Nonlinear Optics, Part 3*; Evans, M., Kielich, S., Eds.; Wiley: New York, 1994; Vol. 85; pp 105−149.

(15) Bouř, P.; Baumruk, V.; Hanzlíková, J. Measurement and Calculation of the Raman Optical Activity of α-Pinene and *trans*-Pinane. *Collect. Czech. Chem. Commun.* **1997**, *62*, 1384–1395.

(16) Hug, W.; Hangartner, G. A Novel High-Throughput Raman Spectrometer for Polarization Difference Measurements. *J. Raman Spectrosc.* **1999**, *30*, 841–852.

(17) Hug, W. Virtual Enantiomers as the Solution of Optical Activity's Deterministic Offset Problem. *Appl. Spectrosc.* **2003**, *57*, 1–13.

(18) Diem, M.; Photos, E.; Khouri, H.; Nafie, L. Vibrational Circular Dichroism in Amino Acids and Peptides. 3. Solution- and Solid-Phase Spectra of Alanine and Serine. *J. Am. Chem. Soc.* **1979**, *101*, 6829–6837.

(19) Freedman, T. B.; Spencer, K. M.; Ragunathan, N.; Nafie, L. Vibrational Circular Dichroism of (*S*,*S*)-[2,3-$^2H_2$]oxirane in the Gas Phase and in Solution. *Can. J. Chem.* **1991**, *69*, 1619–1629.

(20) Lindner, M.; Schrader, B.; Hecht, L. Raman Optical Activity of Enantiomorphic Single Crystals. *J. Raman Spectrosc.* **1995**, *26*, 877–882.

(21) Barron, L. D.; Johnston, C. J. Rotational Raman Optical Activity in Chiral Symmetric Tops. *J. Raman Spectrosc.* **1985**, *16*, 208–218.

(22) Bouř, P.; Tam, C. N.; Wang, B.; Keiderling, T. A. Rotationally Resolved Magnetic Vibrational Circular Dichroism. Experimental Spectra and Theoretical Simulation for Diamagnetic Molecules. *Mol. Phys.* **1996**, *87*, 299–318.

(23) Polavarapu, P. L. The Absolute Configuration of Bromochlorofluoromethane. *Angew. Chem., Int. Ed.* **2002**, *41*, 4544–4546.

(24) Polavarapu, P. L.; Hecht, L.; Barron, L. D. Vibrational Raman Optical Activity in Substituted Oxiranes. *J. Phys. Chem.* **1993**, *97*, 1793–1799.

(25) Helgaker, T.; Ruud, K.; Bak, K. L.; Joergensen, P.; Olsen, J. Vibrational Raman Optical Activity Calculations Using London Atomic Orbitals. *Faraday Discuss.* **1994**, *99*, 165–180.

(26) Ruud, K.; Helgaker, T.; Bouř, P. Gauge-Origin Independent Density-Functional Theory Calculations of Vibrational Raman Optical Activity. *J. Phys. Chem. A* **2002**, *106*, 7448–7455.

(27) Cheeseman, J. R. *Calculation of Molecular Chiroptical Properties Using Density Functional Theory; CD 2007*; University of Groningen: Groningen, The Netherlands, 2007.

(28) Luber, S.; Reiher, M. Theoretical Raman Optical Activity Study of the β Domain of Rat Metallothionein. *J. Phys. Chem. B* **2010**, *114*, 1057–1063.

(29) Yamamoto, S.; Straka, M.; Watarai, H.; Bouř, P. Formation and Structure of the Potassium Complex of Valinomycin in Solution Studied by Raman Optical Activity Spectroscopy. *Phys. Chem. Chem. Phys.* **2010**, *12*, 11021–11032.

(30) Buděšínský, M.; Daněček, P.; Bednárová, L.; Kapitán, J.; Baumruk, V.; Bouř, P. Comparison of Quantitative Conformer Analyses by Nuclear Magnetic Resonance and Raman Optical Activity Spectra for Model Dipeptides. *J. Phys. Chem. A* **2008**, *112*, 8633–8640.

(31) Daněček, P.; Kapitán, J.; Baumruk, V.; Bednárová, L.; Kopecký, V., Jr.; Bouř, P. Anharmonic Effects in IR, Raman and Raman Optical Activity Spectra of Alanine and Proline Zwitterions. *J. Chem. Phys.* **2007**, *126*, 224513.

(32) Bouř, P.; Michalík, D.; Kapitán, J. Empirical Solvent Correction for Multiple Amide Group Vibrational Modes. *J. Chem. Phys.* **2005**, *122*, 144501.

(33) Papoušek, D.; Aliev, M. R. *Molecular Vibrational/Rotational Spectra*; Academia: Prague, Czech Republic, 1982.

(34) Kapitán, J.; Hecht, L.; Bouř, P. Raman Spectral Evidence of Methyl Rotation in Liquid Toluene. *Phys. Chem. Chem. Phys.* **2008**, *10*, 1003–1008.

(35) Pecul, M.; Lamparska, E.; Cappelli, C.; Frediani, L.; Ruud, K. Solvent Effects on Raman Optical Activity Spectra Calculated Using the Polarizable Continuum Model. *J. Phys. Chem. A* **2006**, *110*, 2807–2815.

(36) Šebek, J.; Kapitán, J.; Šebestík, J.; Baumruk, V.; Bouř, P. L-Alanyl-L-alanine Conformational Changes Induced by pH As Monitored by the Raman Optical Activity Spectra. *J. Phys. Chem. A* **2009**, *113*, 7760–7768.

(37) Blanch, E. W.; Hecht, L.; Barron, L. D. Vibrational Raman Optical Activity of Proteins, Nucleic Acids, and Viruses. *Methods* **2003**, *29*, 196–209.

(38) Frisch, M. J.; Trucks, G. W.; Schlegel, H. B.; Scuseria, G. E.; Robb, M. A.; Cheeseman, J. R.; Scalmani, G.; Barone, V.; Mennucci, B.; Petersson, G. A.; et al. *Gaussian 09*; Gaussian, Inc.: Wallingford, CT, 2009.

(39) Becke, A. D. Density-Functional Thermochemistry. IV. A New Dynamical Correlation Functional and Implications for Exact-Exchange Mixing. *J. Chem. Phys.* **1993**, *98*, 5648–5652.

(40) Klamt, A. COSMO and COSMO-RS. In *The Encyclopedia of Computational Chemistry*; Schleyer, P. R., Allinger, N. L., Clark, T., Gasteiger, J., Kollman, P. A., Schaefer, H. F., III, Schreiner, P. R., Eds.; John Wiley & Sons: Chichester, U.K., 1998; Vol. 1, pp 604−615.

(41) Polavarapu, P. L. *Vibrational Spectra: Principles and Applications with Emphasis on Optical Activity*; Elsevier: Amsterdam, 1998; Vol. 85.
(42) Masri, F. N.; Williams, I. R. I. Program for Calculating Degenerate Raman Bands of Symmetric Tops with an Adaptation for Infrared Band. *Comput. Phys. Commun.* **1970**, *1*, 349–358.
(43) Masri, F. N.; Williams, I. R. I. A Fortran Program for Calculating Degenerate Raman Bands of Symmetric Tops with an Adaptation for Infrared Bands. *Comput. Phys. Commun.* **1971**, *2*, 298.
(44) Bouř, P. *S4*; Academy of Sciences: Prague, 1994−2010.
(45) Daněček, P.; Bouř, P. Comparison of the Numerical Stability of Methods for Anharmonic Calculations of Vibrational Molecular Energies. *J. Comput. Chem.* **2007**, *28*, 1617–1624.